Mechanical Solutions, Inc.
Engineering Analysis, Test & Technology

A System for Conducting Sophisticated Mechanical Tests in Situ with High Energy Synchrotron X-Rays

Final Technical Report

DOE Award Number: DE-SC0004864
Recipient: Mechanical Solutions, Inc.
Project Title: A System for Conducting Sophisticated Mechanical Tests in Situ with High Energy Synchrotron X-Rays
Principal Investigator: Jeremy Weiss

SBIR/STTR RIGHTS NOTICE

Table of Contents

1. Executive Summary

Experiments using diffraction of synchrotron radiation that help scientists understand engineering material failure modes, such as fracture and fatigue, require specialized machinery. This machinery must be able to induce these failure modes in a material specimen while adhering to strict size, weight, and geometric limitations prescribed by diffraction measurement techniques. During this Phase I project, Mechanical Solutions, Inc. (MSI) developed one such machine capable of applying uniaxial mechanical loading to a material specimen in both tension and compression, with zero backlash while transitioning between the two.

Engineers currently compensate for a lack of understanding of fracture and fatigue by employing factors of safety in crucial system components. Thus, mechanical and structural parts are several times bigger, thicker, and heavier than they need to be. The scientific discoveries that result from diffraction experiments which utilize sophisticated mechanical loading devices will allow for broad material, weight, fuel, and cost savings in engineering design across all industries, while reducing the number of catastrophic failures in transportation, power generation, infrastructure, and all other engineering systems.

With an existing load frame as the starting point, the research focused on two main areas: 1) the design of a specimen alignment and gripping system that enables pure uniaxial tension and compression loading (and no bending, shear, or torsion), and 2) development of a feedback control system that is adaptive and thus can maintain a load set point despite changing specimen material properties (e.g. a decreasing stiffness during yield).

2. Phase I Results

MSI designed and fabricated a load frame with an alignment system, and grips designed to transfer both tensile and compressive uniaxial mechanical load to the specimen. The load frame drive train was designed to operate with zero backlash, even during transitions between tension and compression. The resulting load frame is pictured in Figure 1.

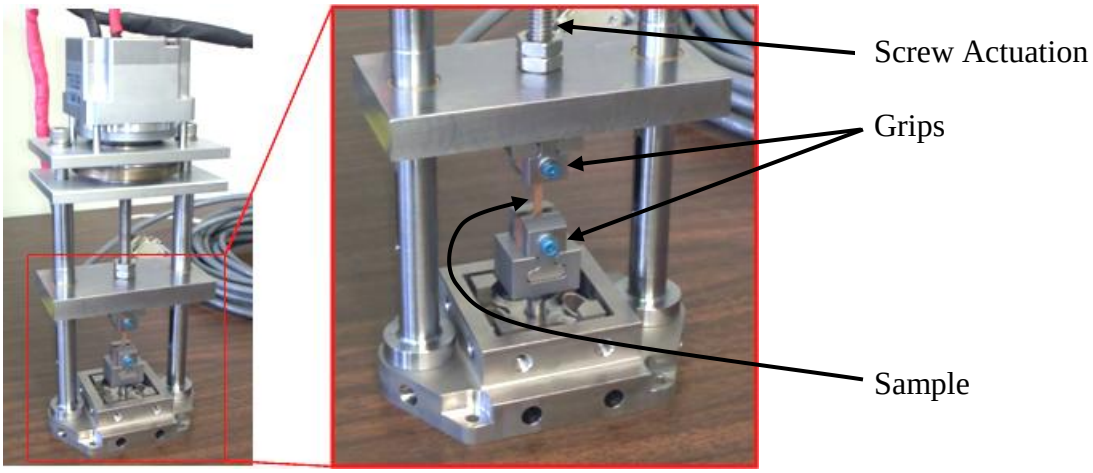

Figure 1: Load frame designed and built during Phase I.

MSI also wrote a feedback control algorithm to maintain load set points while adapting to an evolving specimen stiffness when deformed beyond its linear loading region. This control system was implemented using LabVIEW, with the software interface shown in Figure 2.

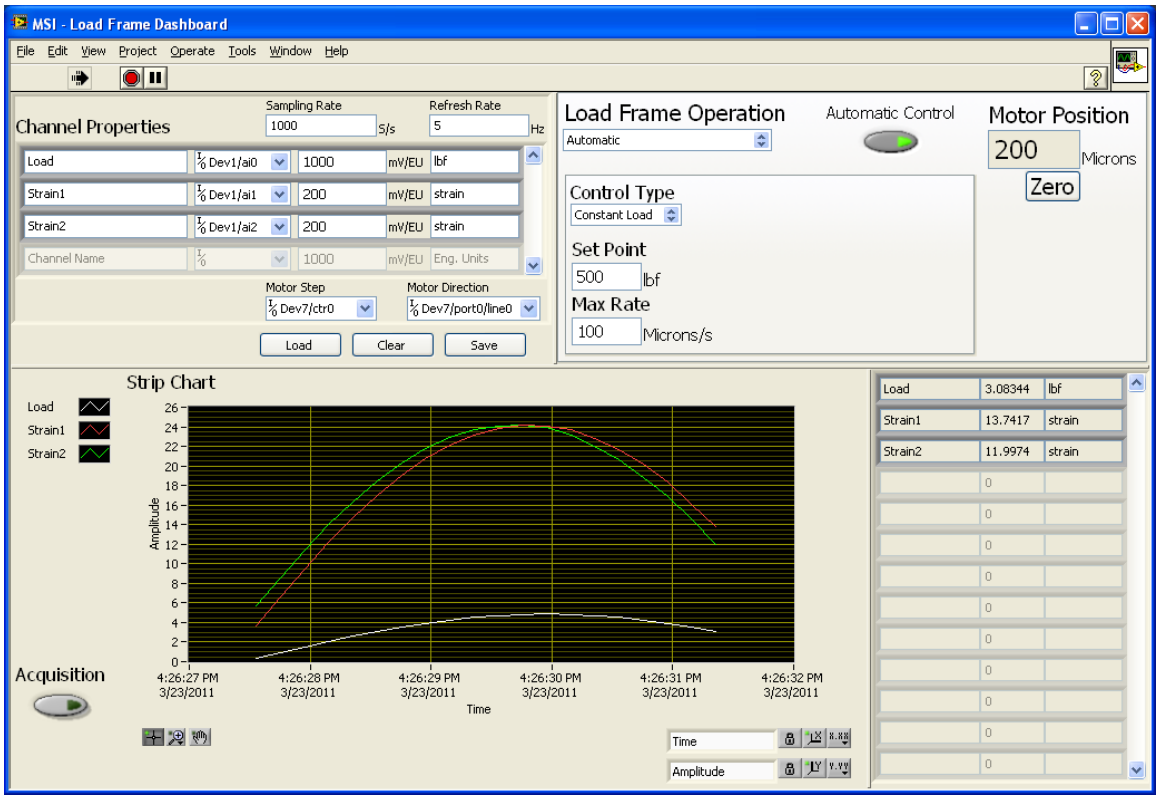

Figure 2: Software interface of the feedback controller used to maintain load set points while adapting to changing material stiffness in the specimen.

The load frame was tested at MSI by cycling an aluminum specimen between tension and compression to confirm load and strain did not dwell at zero for any duration during inversion, which would indicate backlash in the system. Next, the load frame was operated to slowly pull the specimen to failure to be certain that fracture occurred in the gage section and not at the transition to the specimen end. As shown in Figure 3, fracture occurred near the middle of the gage section. Throughout the test, closed-loop control was used successfully to maintain incrementally higher load set points until failure occurred.

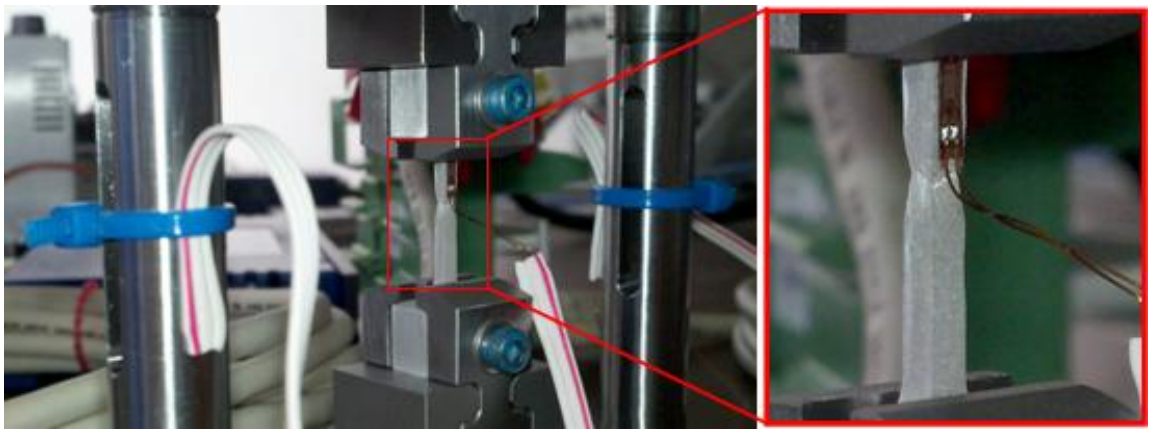

Figure 3: Aluminum specimen after being pulled to failure by the load frame.

The load frame was also tested during x-ray diffraction experiments at the Advanced Photon Source (APS) and Argonne National Laboratory (ANL) in April, 2011. During these experiments, it was found that while the feedback control system generally functioned well, the grip alignment system would need further improvement. It was prohibitively difficult to align small cross section specimen (1mm x 1mm) of soft material (copper) where the alignment process itself was actually capable of yielding the specimen. Larger cross section specimen (2mm x 2mm) could be successfully aligned, but the alignment could not be maintained from one specimen to the next. Each new specimen to be placed in the load frame required alignment, which is impractical during beamtime at a synchrotron facility because of the dense strain gaging required and the time expense. Still, the prototype load frame represents a significant step towards solving the difficult alignment problem that future design iterations will improve on.

3. Phase I Project Activities

3.1. Specimen Design

The first task was to design the material specimen to undergo deformation. The Phase I project builds on an existing load frame design capable of applying 1000 lbf tension or compression, so the specimen must be designed to yield, fatigue, and fracture with sufficient margin to this load. The area of the cross section that would be in compliance with this requirement is dependent on material properties, but 2mm x 2mm was chosen as nominal dimensions. The specimen thickness must also be designed with x-ray penetration in mind, and so 1mm x 1mm is also a cross section option for certain materials.

Because the load frame is intended for use in both tension and compression, the specimen must be designed with buckling in mind. Buckling can spoil a mechanical test, and so it is desired to have a strong margin to buckling based on the specimen cross section and height. MSI used finite element analysis to predict the stress state within various candidate specimen designs, and also predict their critical buckling loads. Figure 4 shows the results for the dimensions that were ultimately selected, using a titanium alloy material properties.

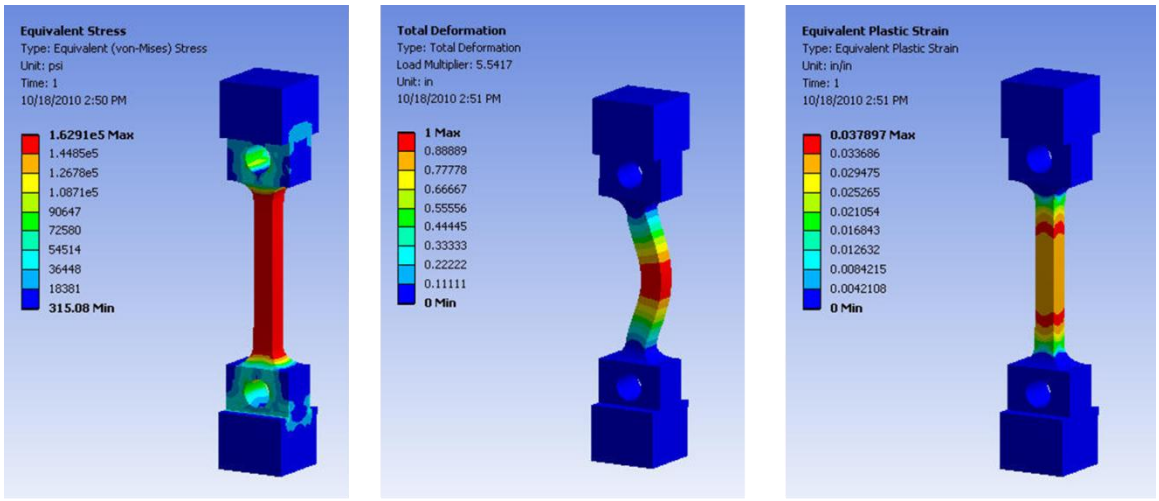

Von-Mises Stress At 1000 lbf Tension (161 ksi through section)

Buckling Analysis Deformation Result ($P_{critical}$ at 5542 lbf)

Plastic Strain at 1000 lbf Tension (0.031 in/in at center)

Figure 4: Results of finite element analysis for stress, buckling, and strain of the specimen design

Finally, the ends of the specimen were designed to interact with the gripping system. The grips must clasp the ends of the specimen with a preload in excess of the largest expected axial load (1000 lbf) to ensure there is no backlash during load inversions. For further discussion, refer to Section 3.3 on grip design.

3.2. Alignment System Design

Parasitic loads from bending, shear, and twist of the specimen are an unfortunate reality and a significant contributor to overall experimental error. These loads arise from the misalignment between the top and bottom grips of the load frame due to imperfect machining and assembly, and result in deformation of the specimen before any axial load is applied. Therefore, MSI designed a gripping system that allows for the measurement of, and correction of, misalignment between the top and bottom grips. The sources of misalignment are illustrated in Figure 5.

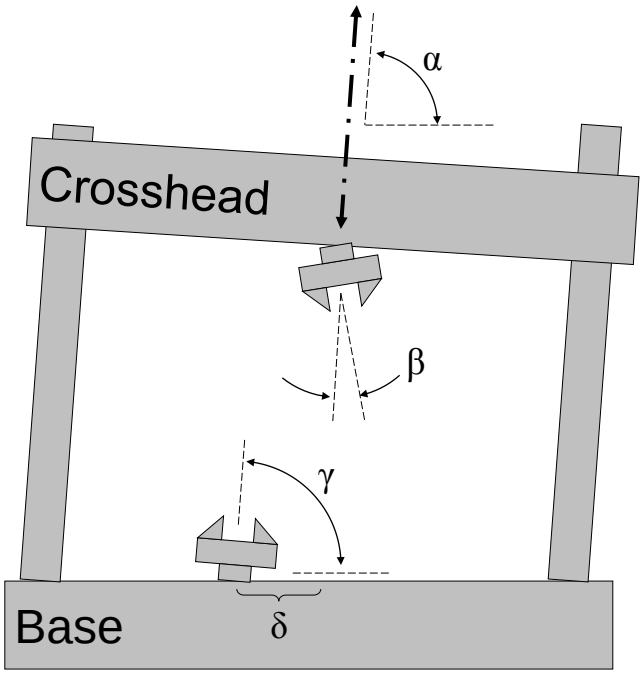

Figure 5: Schematic of the main components of the load frame, with exaggerated sources of misalignment between the top and bottom grips.

In this two-dimensional simplification, angle α defines the direction of travel of the crosshead relative to the plane of the base. Angle β defines the orientation of the top grip relative to the direction of travel of the crosshead. Angle γ represents the orientation of the bottom grip relative to the plane of the base. Finally, distance δ represents the location of the bottom grip relative to the projected location of the top grip.

In MSI's design, and consistent with industry practice, alignment takes take place on the same end of the specimen as the load measurement (bottom), and on the opposite side of the specimen as the actuation (top). Therefore, as the actuation occurs via the crosshead, the load measurement and alignment take place between the base and the bottom grip. Modern machining and assembly techniques can ensure that β is sufficiently close to zero. The alignment task then simplifies to adjusting the bottom grip to minimize δ and align γ as closely as possible with α, which includes twist about the direction of loading. This creates the need for a bottom grip that can translate in the plane of the base and tilt in three directions, and maintain its position and orientation under up to 1000 lbs of axial loading in either direction (tension or compression). With good machining and assembly, the bottom grip would only need adjustment in the range of 0 to 25 mils in any one direction.

The design MSI ultimately developed is shown in Figure 6. In a single body, this part serves as the base, the alignment mechanism, and the load cell adapter. From here on out, it is referred to simply as "the base."

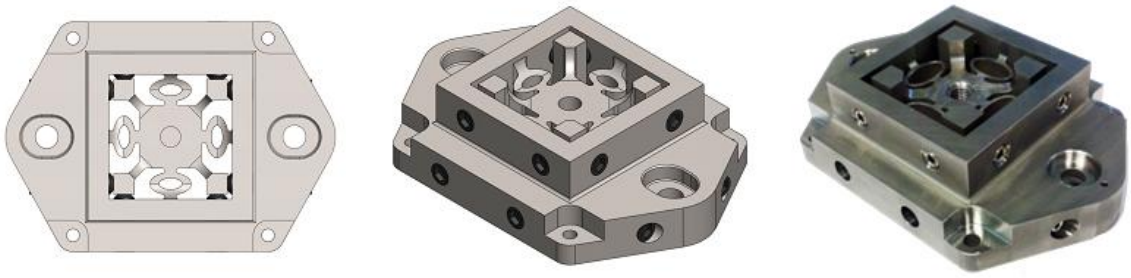

Figure 6: Top and isometric views of the base solid model and manufactured part.

The base consists of a centerpiece with square cross section that attaches to a square annulus via four extruded elliptical annuli. A tapped hole in the middle of the centerpiece receives the load cell. Sixteen setscrews—four per side—adjust the position and orientation of the centerpiece by pushing on the arms protruding from each of corner of the centerpiece. The arms and ellipses elastically deform as dictated by the setscrews to allow translation and rotation of the centerpiece. Two large holes flanking the square annulus hold the guide bars. Four outer holes are for mounting the load frame to a positioning stage or goniometer.

An off-the-shelf load cell with threaded studs forms a rigid connection between the base and the bottom grip. Aligning the bottom grip is a matter of tightening or loosening the appropriate setscrews while an alignment specimen is mounted in the load frame. The alignment specimen has several strain gages affixed to the loading region, as shown in Figure 7.

Figure 7: Alignment specimen with strain gages affixed. When in alignment, all the strain gages should produce the same output.

With the strain gage outputs displayed on an oscilloscope guiding the user, the setscrews are adjusted until all the strain gages measure sufficiently close to zero. For example, to translate the bottom grip, tighten all four screws on one side while loosening the four on the opposite side. The screws that were tightened now push against their respective spokes, which deform as well as transfer a lateral force on the centerpiece. The elasticity of the spokes allows for fine control over the displacement of the centerpiece. All four ellipses also deform to allow for the displacement, with one compressing, one elongating, and two shearing.

To achieve tilt and twist, similar action is required. By tightening and loosening the appropriate combination of setscrews, the spokes will deform as prescribed while transferring a force to the centerpiece. The centerpiece will shift while deforming all four ellipses accordingly. The ellipses were engineered to provide ample flexibility in the horizontal plane while remaining sufficiently stiff in the direction of loading. MSI used finite element analysis to ensure the ellipses will not buckle or fatigue.

3.3. Grip Design

A mechanism for transferring load to the specimen was needed that allows for compression, tension, and zero backlash transition between the two. To ensure no dead zone during load inversions, the ends of the specimen are preloaded within the grips. To be effective, the preload must exceed the applied tensile or compressive load, in this case 1000 lbf. This preload is isolated to the ends of the specimen; the gage section only experiences the applied load as prescribed by the translation of the crosshead. For compatibility with diffraction measurements, achieving the preload within the smallest possible package will ensure minimal shadowing of incoming and outgoing X-rays.

Shown in Figure 8, MSI's design features two jaws that travel inward along T-slots to clamp around the end of the specimen. A threaded pin passes through a hole in the specimen end, with radial clearance, and pulls the jaws inward against the sloped faces of the specimen end. The tension that builds in the pin from its tightening translates, via those sloped faces, into a compressive preload on the specimen end. The threaded pin maintains radial clearance throughout, and does not carry any other load besides tension used for preloading. A stud is used to locate the specimen relative to the grip to ensure the centroidal axes of the grip and specimen are collinear.

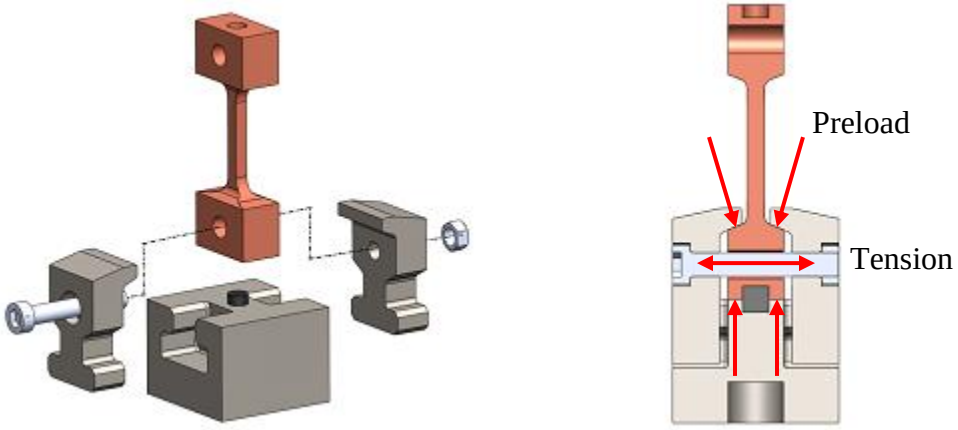

Figure 8: Exploded and cutaway views of the gripping system illustrate how the ends of the specimen are preloaded to eliminate backlash during inversion between tension and compression.

The angle of the sloped faces of the specimen end was engineered to produce the most compressive preload for the least amount of tension in the threaded pin. The pin diameter includes a factor of safety to ensure it can withstand the tension required for preloading. Finite element analysis was used to simulate the stresses in all parts of the gripping system due to the preload as well as due to the applied load. The parts were analyzed for stiffness, yield, and where appropriate, fatigue. It should be noted that the specimen ends

are sufficiently compact to enable characterization by near-field diffraction techniques prior to *in situ* far-field examination in the load frame.

Figure 9 shows a free body diagram of the preloaded grip system. The system is comprised of a sample end, a base, two grips, and a pin. The tension in the pin, F_P, is increased via threads. The reaction force from the tension pushes each grip inward toward the sample end. The top of each grip interacts with the sloped faces of the sample end creating the downward preload, F_B.

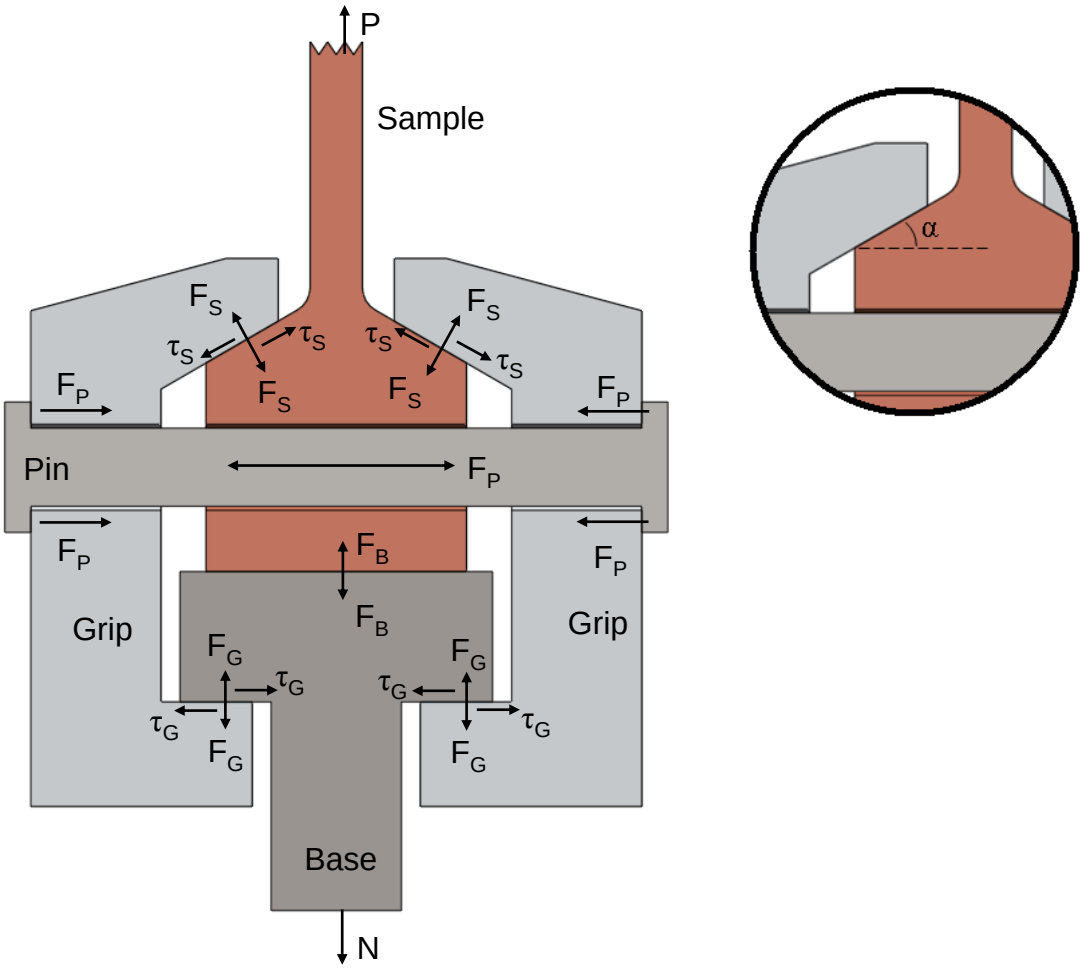

Figure 9: Free Body Diagram of preloaded grip design.

The following forces and parameters are considered in the Free Body Diagram:

- **F_P** – Force between the Pin and the Grip, caused by tension in the Pin by tightening its threads
- **F_S, τ_S** – Normal force and tangential friction force between the Grip and the Sample

- **F_B** – Force between the Grip and the Base; this represents the preload and should never change direction during an experimental, even if P cycles from positive to negative
- **F_G, τ_G** – Normal force and tangential friction force between the Grip and the Base
- **P** – Applied load on Sample
- **N** – Normal force from load frame base
- **μ_1** – Coefficient of static friction between the sample and the grip
- **μ_2** – Coefficient of static friction between the base and the grip
- **α** – Angle of the sloped face of the end of the specimen

A preload of at least 1000 lbs is required on each end of the specimen to prevent backlash during load inversion. Only the ends of the specimen will be preloaded; the gage section will only experience P during mechanical testing. It is desired to achieve this preload with the smallest possible tension in the pin. To calculate the preload, F_B, in terms of the tension in the pin, F_P, first consider the horizontal forces on the left grip, as in Equation 1.

$$\sum F_X = F_P - F_s \sin\alpha - \tau_S \cos\alpha - \tau_G = 0 \qquad \text{Eq. 1}$$

Next, consider the vertical forces on the sample, as in Equation 2.

$$\sum F_Y = P + F_B + 2\tau_S \sin\alpha - 2F_S \cos\alpha = 0 \qquad \text{Eq. 2}$$

Expressing the frictional forces in terms of their respective coefficients of friction and normal forces yields Equations 3a and 3b.

$$\tau_S = \mu_1 F_S \qquad \text{Eq. 3a}$$
$$\tau_G = \mu_2 F_G \qquad \text{Eq. 3b}$$

Plugging these expressions into Equations 1 and 2 gives Equations 4 and 5, respectively.

$$F_P - F_s \sin\alpha - \mu_1 F_S \cos\alpha - \mu_2 F_G = 0 \qquad \text{Eq. 4}$$
$$P + F_B + 2\mu_1 F_S \sin\alpha - 2F_S \cos\alpha = 0 \qquad \text{Eq. 5}$$

Next, F_G can be expressed in terms of the preload, F_B, and the applied load, P, by first considering the vertical forces on the base, as in Equation 6.

$$\sum F_Y = 2F_G - F_B - N = 0 \qquad \text{Eq. 6}$$

It can be shown that the reaction force on the base, N, is equal to the applied load, P, by considering only the external forces on the entire system in equilibrium. With this information and Equation 6, F_G can be expressed more usefully in terms of the preload and the applied load, as in Equation 7.

$$F_G = \frac{F_B + P}{2} \qquad \text{Eq. 7}$$

Updating Equation 4 to include this expression gives Equation 8.

$$F_P - F_s \sin\alpha - \mu_1 F_S \cos\alpha - \mu_2\left(\frac{F_B + P}{2}\right) = 0 \qquad \text{Eq. 8}$$

Equations 5 and 8 represent a system of two equations and two unknowns, F_S and F_B, with known input parameters P, α, μ_1, μ_2, and F_P. Algebraic manipulation provides equations for F_B and F_S, shown in Equations 9 and 10, respectively.

$$F_B = \frac{2F_P(\cos\alpha - \mu_1 \sin\alpha)}{\sin\alpha + \mu_1 \cos\alpha + \mu_2(\cos\alpha - \mu_1 \sin\alpha)} - P \qquad \text{Eq. 9}$$

$$F_S = \frac{F_P}{\sin\alpha + \mu_1 \cos\alpha + \mu_2(\cos\alpha - \mu_1 \sin\alpha)} \qquad \text{Eq.10}$$

Using the equation for F_B, F_G can also be expressed in terms of known inputs parameters, as shown in Equation 11.

$$F_G = \frac{F_P}{\sin\alpha + \mu_1 \cos\alpha + \mu_2(\cos\alpha - \mu_1 \sin\alpha)} \qquad \text{Eq. 11}$$

There are two important points to note. First, the external load, P, does not appear in the equations for the force between the grip and the sample or the force between the grip and the base. These forces are solely dependent on the tension in the pin, the geometry of the end of the sample, and on the frictional properties between the various components. Second, F_B, is very much dependent on the applied load P. When the applied load is tensile, F_B will decrease. Appropriate preload (1000 lbs) should be used to ensure that F_B never becomes negative, which would be indicative of backlash. When the applied load is compressive, F_B will increase.

The angle of the sloped face of the end of the specimen translates the horizontal tension in the pin into a downward preload on the sample. This angle should be chosen to achieve as much preload "output" for a given pin tension "input." To this end, it is helpful to define a mechanical advantage between the preload and the pin tension while there is no applied load (P = 0), as in Equation 12.

$$\eta = \frac{F_B}{F_P} = \frac{2(\cos\alpha - \mu_1 \sin\alpha)}{\sin\alpha + \mu_1 \cos\alpha + \mu_2(\cos\alpha - \mu_1 \sin\alpha)} \qquad \text{Eq. 12}$$

Figure 10 through Figure 12 shows graphs of η as a function of α for various combinations of likely coefficients of friction.

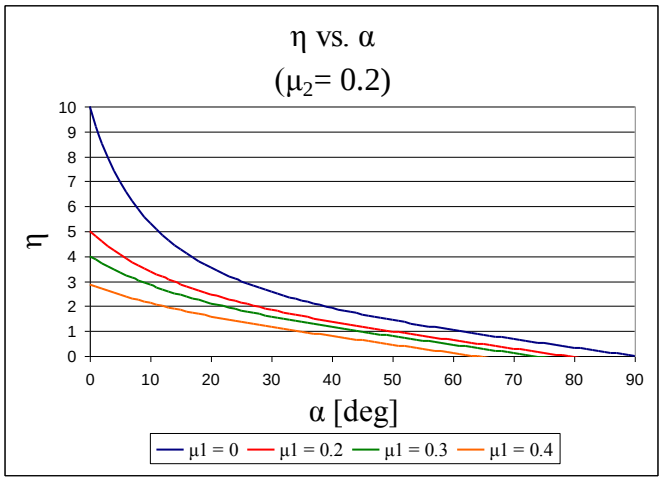

Figure 10: Mechanical advantage as a function of the angle of the end of the sample for $\mu_2 = 0.2$

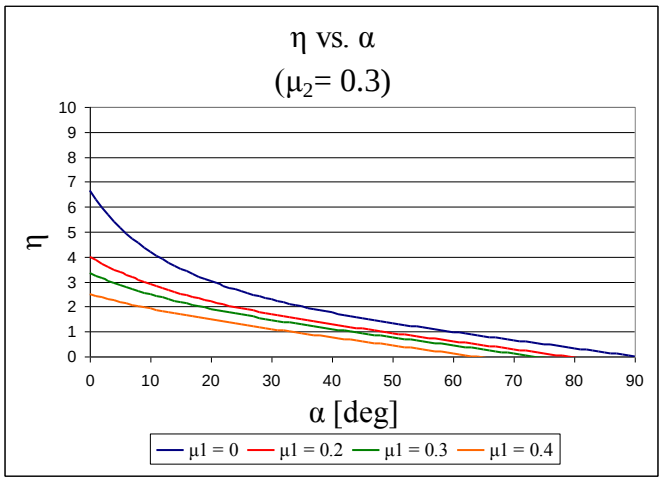

Figure 11: Mechanical advantage as a function of the angle of the end of the sample for $\mu_2 = 0.3$

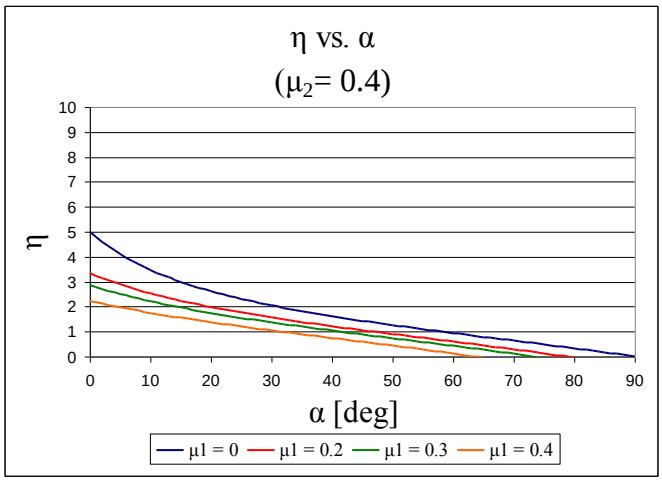

Figure 12: Mechanical advantage as a function of the angle of the end of the sample for $\mu_2 = 0.4$

The Figures show that regardless of the coefficients of friction, a smaller angle on the end of the specimen provides a higher preload for the same pin tension. It appears entirely possible that a couple hundred pounds of tension in the pin will easily translate into a 1000 lbf preload on the sample. Seemingly, at 0°, there is unlimited mechanical advantage and an infinitesimal pin tension will create an infinite preload. Of course, this is not possible. The drawback to a small angle is that the above analysis becomes more sensitive to the true dimensions of each part. Indeed, at 0°, the grips would have to travel an infinite length to initiate contact with the sloped faces of the end of the sample.

Therefore, the best value for α will be a compromise between mechanical advantage and what dimensional tolerances are reliably achievable. Ultimately, 22.5° was chosen because it provides a good mechanical advantage at a sufficiently large angle.

3.4. Feedback Control Algorithm Development

The adaptive feedback control algorithm was based on a simplified model of the test specimen. Consider the specimen as a spring with stiffness *k* that is rigidly fixed to the base at one end, and attached to the moveable crosshead at the other, as depicted in Figure 13. The stiffness will remain approximately constant while the specimen is deformed elastically. Beyond a certain displacement, the stiffness will then vary nonlinearly based on elongation, load rate, the deformation history, and other variables.

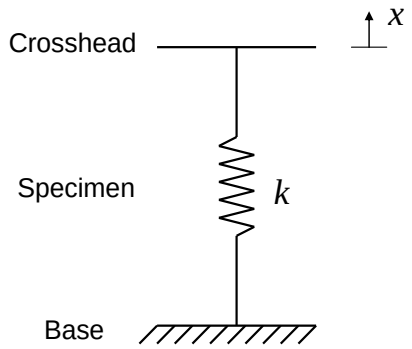

Figure 13: Idealized model of the specimen during a mechanical test.

If the stiffness is known, then maintaining a load set point is a matter of measuring the load error (desired minus measured), and computing the displacement required to make up the difference using Hooke's law. Moving the crosshead by this amount should reduce the load error to zero. Repeating this process in a loop provides the basis for the algorithm for a closed-loop controller.

As recently mentioned, though, the stiffness quickly becomes an unknown once the specimen is deformed beyond its yield point. Therefore, the control algorithm must adapt to the changing stiffness using information from previous loop iterations: specifically, how much did the crosshead just move, and how did that movement affect the measured load? Within each loop iteration, this information can be used to compute the "local" specimen stiffness, and subsequently, the required crosshead displacement to zero any

load error. To reject noise and outliers, a moving average of the "local" stiffness can be used, comprised of the mean of the last handful of values. So long as the algorithm iterates at a considerably faster rate than the material stiffness can change, the load frame will sufficiently maintain the load set point.

However, there is the possibility that the next loop iteration will commence before the motor has had the chance to complete the required displacement from the previous iteration. The algorithm must gracefully handle this possible situation, known as saturation, which occurs when the measured load is far from the desired load. If the controller is cognizant of the maximum crosshead displacement achievable in one loop iteration, which depends on the motor rate and the loop rate, then it can limit the displacement command sent to the load frame motor. If the load error requires a larger displacement than can be achieved in one iteration, the maximum achievable movement is instead executed, and the situation reassessed on the next iteration.

The conceptual algorithm described above is suitable for both constant and cyclically varying set points, and can also be used to smoothly travel between set points. Because of how it deals with saturation, the crosshead will rise or fall at a constant rate until the load error is below a critical value, at which point the system is no longer saturated. Achieving cyclical loading simply requires alternating the set point between a minimum and maximum value at a user-defined frequency.

LabVIEW communicates with the load frame motor using TTL pulse trains and logic. The motor and ACME lead screw combine to give an extraordinary resolution of 1.76 nanometers of vertical crosshead motion per TTL pulse. After the feedback loop computes a displacement, it then converts this from a length to a quantity of pulses. A zero-to-five volt pulse train of the appropriate length is output to the stepper motor circuitry which results in the required movement of the crosshead.

4. Products Developed

4.1. Load Frame

Hardware resulting from the Phase I effort includes the load frame, pictured in Figure 1. The base, grips, guide bars, crosshead, and motor support bracket were fabricated by local machinists. The motor, lead screw, and motor nut were borrowed from an existing load frame in service at APS. The load cell was purchased off-the-shelf.

4.2. Feedback Controller

Software resulting from Phase I includes the adaptive feedback control algorithm, implemented using LabVIEW, and pictured in Figure 2.